
Article:
Imada, K. orcid.org/0000-0002-8128-2438, Wilson, H. R. orcid.org/0000-0003-3333-7470, Connor, J. W. et al. (2 more authors) (2018) Drift kinetic response of ions to magnetic island perturbation and effects on NTM threshold. Journal of Physics: Conference Series. 012013. ISSN: 1742-6596

https://doi.org/10.1088/1742-6596/1125/1/012013

Drift kinetic response of ions to magnetic island perturbation and effects on NTM threshold

IOP Conf. Series: Journal of Physics: Conf. Series **1125** (2018) 012013 doi:10.1088/1742-6596/1125/1/012013

Drift kinetic response of ions to magnetic island perturbation and effects on NTM threshold

K Imada[1], H R Wilson[1,2], J W Connor[2], A V Dudkovskaia[1] and P Hill[1]

[1] York Plasma Institute, Department of Physics, University of York, Heslington, York, YO10 5DD, United Kingdom
[2] CCFE, Culham Science Centre, Abingdon, Oxon, OX14 3DB, United Kingdom

Abstract. Controlling neoclassical tearing modes (NTMs) is vital for future tokamaks, such as ITER. An NTM control system relies on the magnetic island threshold physics. In this paper, new results for the ion response to the island perturbation and its influence on the island evolution are presented. Considering a small island, $w \ll r$, where r is the minor radius, but crucially retaining the ordering $\rho_{bi} \sim w$ (relevant for threshold) to capture the finite orbit width effect, we determine the ion response using the drift kinetic equation. Momentum conservation and quasineutrality are taken into account, which are crucial for determining the current perturbations. The results show that the finite particle orbit effects are significant even for a moderately small ratio of $\rho_{\theta i}/w$ ($\rho_{\theta i}$ is the ion poloidal Larmor radius; $\rho_{bi} \sim \epsilon^{1/2}\rho_{\theta i}$). When $w \sim \rho_{\theta i}$, the flattening of the pressure gradient across the island is substantially restored, implying that the bootstrap current drive for the island growth is suppressed. Moreover, we find that for a sufficiently small island, $w \ll \rho_{\theta i}$, the contribution can be negative, meaning that it can stabilize small seed islands, providing a threshold. This will have significant impact on our understanding of the NTM threshold physics.

1. Introduction

One of the challenges that future tokamaks will face is the effect of neoclassical tearing modes (NTMs), which are characterized by the evolution of a magnetic island chain. Across a magnetic island the enhanced radial transport of particles and heat flattens the pressure gradient, degrading the plasma confinement. NTMs with large saturated islands can trigger disruptions. This is why it is important to control NTMs.

According to the original Rutherford theory [1], the evolution of a magnetic island half-width, w, depends on the tearing parameter, Δ'. In neoclassical theory, the contribution from a localized parallel current perturbation is taken into account. One such contribution is the perturbed bootstrap current [2], whose contribution to the island evolution (which we label Δ_{bs}) scales as $1/w$. It means that, if this is destabilizing, seed islands, however small, would grow to large saturated ones, significantly degrading tokamak confinement. However, experimental observations point to a threshold mechanism [3], whereby sufficiently small islands heal themselves and shrink away. One possible source of this threshold is the finite radial transport effect [4, 5]. This partially restores the pressure gradient that is flattened across the island, thus reducing the bootstrap drive for the island growth. In this case, the island growth below a critical width is suppressed.

In toroidal geometry, the combination of $\boldsymbol{\nabla} B$ and curvature drifts causes the particle orbits to stray from a reference flux surface by a distance $\sim \epsilon\rho_\theta$ for passing particles (ρ_θ is the poloidal Larmor radius), while trapped particles execute closed banana orbits, whose width is given by $\rho_b \sim \epsilon^{1/2}\rho_\theta$. When an island chain propagates through the plasma, the different orbit-averaged $\mathbf{E} \times \mathbf{B}$ drifts of trapped ions and electrons result in a net current: the neoclassical polarization current. A parallel return current flows to satisfy $\boldsymbol{\nabla} \cdot \mathbf{J} = 0$, and it is this current that contributes to the island evolution (which we label Δ_{pol}). Previous works [6, 7] based on drift kinetic theory

in toroidal geometry have shown that $\Delta_{pol} \propto 1/w^3$, when $\rho_{bi} \ll w$. If this contribution is stabilizing, then it could heal small seed islands, thus providing the threshold.

The currently favoured way of controlling NTMs in ITER is to use electron-cyclotron current drive (ECCD) [8, 9, 10]. Although the effectiveness of the ECCD has been demonstrated in a number of tokamaks [11, 12, 13, 14], the power consumption of the ECCD system is rather high. It is therefore crucial to maximize the efficiency of the system, if we are to achieve a high fusion Q-factor in future experiments [15]. This is why the understanding of the NTM threshold physics, including the predictive capability for the threshold island width, is so essential. Existing theory relies on the assumption $\rho_{bi} \ll w$, i.e. valid in the limit of large island widths compared to the ion banana width. However, observations [16] show that the threshold island width is often comparable in size to the ion banana width; precisely the regime where this assumption breaks down. A new theory is therefore required to accurately determine the relative sizes of the Δ_{bs}, Δ_{pol} and Δ' contributions, including their dependence on the curvature and finite particle orbit width effects. This will allow us to quantitatively predict the threshold width for ITER.

This paper focuses on the effect of finite ion orbit width on the bootstrap current contribution to the magnetic island evolution, extending the existing drift kinetic theory [6] to describe the ion response to the island perturbation. Crucially we relax the small banana-width assumption, and consider magnetic islands whose widths are comparable to the ion banana width: $w \sim \rho_{bi}$. We consider a small magnetic island $w \ll r$ (valid for an island with a width close the threshold width), which allows us to treat the plasma as toroidally symmetric to leading order. Then, because of the finite orbit width effect, the ion distribution function is no longer a function of poloidal magnetic flux ψ, but of toroidal canonical angular momentum:

$$p_\phi = (\psi - \psi_s) - \frac{I v_\parallel}{\omega_{ci}}, \tag{1}$$

which is conserved along the orbits in an axisymmetric plasma. Here, ψ_s is the poloidal flux at the rational surface where the island is located, $I = RB_\phi$, B_ϕ is the toroidal component of the magnetic field, $v_\parallel$ is the component of the particle velocity along the field lines and ω_{ci} is the ion gyrofrequency. For electrons, the assumption $\rho_{be} \ll w$ is still valid, which allows us to use the existing analytic solutions for the electron distribution function of [6]. However, in the regime $\rho_{be} \ll w \sim \rho_{bi}$, we anticipate a notable difference in the electron and ion distribution functions, if we neglect the electrostatic potential Φ. Indeed, one of our findings is that the ion density gradient will be supported across the island when $w \sim \rho_{\theta i}$ (N.B. $\rho_{bi} \sim \rho_{\theta i}$), even if the electron density is still flat (i.e. without the potential). It is therefore important to calculate Φ self-consistently from quasineutrality, which we incorporate into our analysis. From the particle responses, we determine the full contribution of the perturbed current to the island evolution including the bootstrap current. We will find that, in the limit of a very small island, the electrons provide the stabilizing contribution; not explained by the standard bootstrap theory.

2. Magnetic Island Geometry and Drift Kinetic Equation

We consider a large aspect ratio, circular cross-section tokamak, neglecting the Shafranov shift. In the orthogonal coordinate system $\boldsymbol{\nabla}\phi \times \boldsymbol{\nabla}\psi = rB_\theta \boldsymbol{\nabla}\theta$, where ψ is the poloidal magnetic flux, θ is the poloidal angle, ϕ is the toroidal angle and B_θ is the poloidal magnetic field, the equilibrium magnetic field is given by:

$$\mathbf{B}_0 = I(\psi)\boldsymbol{\nabla}\phi + \boldsymbol{\nabla}\phi \times \boldsymbol{\nabla}\psi. \tag{2}$$

A magnetic perturbation of the following form, which satisfies $\boldsymbol{\nabla} \cdot \mathbf{B} = 0$, is introduced:

$$\mathbf{B}_1 = \boldsymbol{\nabla} \times (A_\parallel \boldsymbol{b}_0), \quad A_\parallel = -\frac{\tilde{\psi}}{R}\cos\xi \tag{3}$$

assuming a single dominant helicity perturbation. Here, $\boldsymbol{b}_0 = \mathbf{B}_0/B_0$ is the unit vector in the direction of the equilibrium field lines and ξ is the helical angle in the island rest frame:

$$\xi = m\left(\theta - \frac{\phi}{q_s}\right). \tag{4}$$

m is the poloidal mode number, $q_s = m/n$ is the safety factor at the rational surface where the island is located and n is the toroidal mode number. All quantities with subscript s are those evaluated at the rational surface, unless otherwise indicated. In equation (3), $\tilde{\psi} = (w_\psi^2/4)(q_s/q_s')$ describes the perturbation amplitude, with the prime denoting a differential with respect to ψ. Here, w_ψ is the island half-width in ψ-space. It is also convenient to introduce a perturbed flux function Ω satisfying: $\mathbf{B}\cdot\boldsymbol{\nabla}\Omega = 0$, which is given by:

$$\Omega = \frac{2(\psi-\psi_s)^2}{w_\psi^2} - \cos\xi. \tag{5}$$

The perturbed magnetic field lines lie in surfaces of constant Ω, with $\Omega = 1$ defining the island separatrix.

We consider a steady state drift kinetic response of ions to the magnetic island perturbation. Working in the island rest frame, the drift kinetic equation we employ takes the form:

$$v_\parallel \nabla_\parallel f_j + \boldsymbol{v}_E\cdot\boldsymbol{\nabla} f_j + \boldsymbol{v}_b\cdot\boldsymbol{\nabla} f_j - \frac{e_j}{m_j v}\left(v_\parallel\nabla_\parallel\Phi + \boldsymbol{v}_b\cdot\boldsymbol{\nabla}\Phi\right)\frac{\partial f_j}{\partial v} = C_j(f_j) \tag{6}$$

for a particle species j. Here, $\parallel$ denotes a component parallel to the magnetic field lines, $\nabla_\parallel = \boldsymbol{b}\cdot\boldsymbol{\nabla}$, $\boldsymbol{b} = \mathbf{B}/B$, $v_\parallel = \sigma v\sqrt{1-\lambda B}$ is the parallel velocity, $\boldsymbol{v}_E = (\mathbf{B}\times\boldsymbol{\nabla}\Phi)/B^2$ is the $\mathbf{E}\times\mathbf{B}$ drift, $\boldsymbol{v}_b = -v_\parallel\boldsymbol{b}\times\boldsymbol{\nabla}(v_\parallel/\omega_{cj})$ is the combination of grad-B and curvature drifts, $\omega_{cj} = e_jB/m_j$ and e_j and m_j are the particle charge and mass respectively. Φ is the perturbed electrostatic potential, to be determined from quasineutrality, and C_j is the momentum-conserving model collision operator [17]. Like-like particle and electron-ion collision operators are respectively given by:

$$C_{jj}(f) = 2\nu_{jj}(v)\left[\frac{\sqrt{1-\lambda B}}{B}\frac{\partial}{\partial\lambda}\left(\lambda\sqrt{1-\lambda B}\frac{\partial f}{\partial\lambda}\right) + \frac{v_\parallel\bar{u}_{\parallel j}}{v_{thj}^2}F_{Mj}\right], \tag{7}$$

$$C_{ei}(f) = 2\nu_{ei}(v)\left[\frac{\sqrt{1-\lambda B}}{B}\frac{\partial}{\partial\lambda}\left(\lambda\sqrt{1-\lambda B}\frac{\partial f}{\partial\lambda}\right) + \frac{v_\parallel u_{\parallel i}}{v_{the}^2}F_{Me}\right], \tag{8}$$

where the λ differentials are taken at fixed ψ. $\bar{u}_{\parallel j}$ is required for momentum conservation:

$$\bar{u}_{\parallel j}(f) = \frac{1}{n\langle\nu_{jj}\rangle_v}\int d\boldsymbol{v}^3\ \nu_{jj}v_\parallel f. \tag{9}$$

(See [17] for the definitions of the deflection frequency $\nu_{jj}(v)$ and velocity integral $\langle\nu_{jj}\rangle_v$.)

In equation (6), spatial derivatives are taken at constant kinetic energy, $\mathcal{E} = v^2/2$, and magnetic moment, $\mu = v_\perp^2/2B$ where $\perp$ denotes a component perpendicular to magnetic field lines. In Section 5, when the current perturbation is calculated, the analytic result for the electron response in the limit of $\rho_{be} \ll w$ [6] is used. However, it is worthwhile pointing out that the electron flow depends on the ion counterpart through momentum conservation, as is indicated by equation (8). The electron flow is then given by:

$$\frac{\left\langle\langle Bu_{\parallel e}\rangle_\theta\right\rangle_\Omega}{B_0v_{the}} = -\frac{f_t}{(1+f_t)}\frac{Iv_{the}}{\omega_{ce}}\frac{n'}{n}\left(1+\eta_e+\frac{1}{2}kf_c\eta_e\right)\left\langle\frac{\partial h}{\partial\psi}\right\rangle_\Omega + \frac{f_c}{(1+f_t)}\frac{\left\langle\langle Bu_{\parallel i}\rangle_\theta\right\rangle_\Omega}{B_0v_{thi}}, \tag{10}$$

where $\langle ... \rangle_\Omega$ describes the flux surface-average:

$$\langle \cdots \rangle_\Omega = \frac{\oint \cdots [\sqrt{\Omega + \cos\xi}]^{1/2}\, d\xi}{\oint [\sqrt{\Omega + \cos\xi}]^{1/2}\, d\xi}. \tag{11}$$

In equation (10) f_c and f_t are the passing and trapped particle fractions respectively, $k = -1.173$ [18], $\eta_j = (T_j'/T_j)/(n'/n)$ and $h(\Omega)$ describes the perturbed density profile in the vicinity of an island:

$$h(\Omega) = \Theta(\Omega - 1)\frac{w_\psi}{2\sqrt{2}} \int_1^\Omega \frac{d\Omega'}{Q(\Omega')}, \quad Q(\Omega) = \frac{1}{2\pi}\oint \sqrt{\Omega + \cos\xi}. \tag{12}$$

3. Ion Response

While we assume $\rho_{\theta e} \ll w$ for electrons, for ions we consider the case where the ion poloidal Larmor radius is comparable to the island width. Relaxing the assumption $\rho_{\theta i} \ll w$, we seek a Maxwellian solution for the ion distribution function, and Taylor-expand it in the vicinity of the rational surface, $\psi = \psi_s$, in the small island limit, $w \ll r$. Then the ion distribution function can be written as:

$$f_i = \left(1 - \frac{Ze\Phi}{T_i}\right) F_{Mis} + G_i, \tag{13}$$

where $F_{Mi} = (n_0/\pi^{3/2} v_{thi}^3) \exp[-v^2/v_{thi}^2]$ is the Maxwellian, and $v_{thi}^2 = 2T_i/m_i$. Using the parameter $\Delta = w/r \ll 1$, we expand the perturbation in the ion distribution function in terms of Δ, retaining the ordering $\rho_{\theta i} \sim w$:

$$G_i = \sum_k \Delta^k G_k. \tag{14}$$

When $\rho_{\theta i} \sim w$, both parallel streaming and magnetic drift dominate the ion response. Then, the leading order contributions to the drift kinetic equation (6) are:

$$\frac{v_\parallel}{Rq}\left[\left.\frac{\partial G_0}{\partial\theta}\right|_\psi + I\frac{\partial}{\partial\theta}\left(\frac{v_\parallel}{\omega_{ci}}\right)\frac{\partial G_0}{\partial\psi}\right] = 0. \tag{15}$$

In the limit of $w \ll r$, the toroidal symmetry is approximately conserved to the leading order in Δ. Then the toroidal canonical momentum (1) is a conserved quantity along particle orbits, which we can utilize as a radial coordinate in place of ψ. As we shall see, this allows us to eliminate one of the spatial coordinates, θ. Thus, transforming from radial variable ψ to p_ϕ, equation (15) simplifies to:

$$\frac{v_\parallel}{Rq}\left.\frac{\partial G_0}{\partial\theta}\right|_{p_\phi} = 0, \tag{16}$$

which can straightforwardly be integrated to yield:

$$G_0 = \bar{G}_0(p_\phi, \xi, \boldsymbol{v}). \tag{17}$$

This result for G_0 means that the distribution function is a constant on the orbits the particles free-stream along, rather than being a flux surface quantity. These orbits are described by p_ϕ =constant (i.e. the standard neoclassical orbits for a toroidally symmetric system).

We now proceed to the $O(\Delta)$ contribution to the drift kinetic equation (6). In order to annihilate the term in G_1, for passing particles we multiply the $O(\Delta)$ equation by $Rq/v_\parallel$ and integrating over a period in θ at fixed p_ϕ, making use of the periodicity in G_1. For trapped particles, the distribution functions at the bounce points satisfy: $G_1(\sigma = +1, \theta_b = \pm 1) =$

$G_1(\sigma=-1,\theta_b=\pm1)$, by conservation of particles. Thus, the term in G_1 for trapped particles can be eliminated by multiplying the $O(\Delta)$ equation by $Rq/|v_\parallel|$, summing over σ and then integrating with respect to θ between the bounce points. The result is a particle orbit-averaged equation for $\bar{G}_0$. Introducing normalized quantities:

$$x=\frac{\psi-\psi_s}{\psi_s},\quad y=\lambda B_{\max},\quad \hat{v}=\frac{v}{v_{thi}},\quad \hat{p}=\frac{p_\phi}{\psi_s},\quad b=\frac{B(\theta)}{B_{\max}}=\frac{1-\epsilon\cos\theta}{1+\epsilon},$$
$$\hat{L}_q^{-1}=\frac{\psi_s}{q_s}\left.\frac{dq}{d\psi}\right|_s,\quad \hat{L}_n^{-1}=\frac{\psi_s}{n}\frac{dn}{d\psi},\quad \hat{L}_B^{-1}=\frac{\psi_s}{B}\frac{\partial B}{\partial\psi},\quad \hat{w}=\frac{w}{r_s},\quad \hat{\rho}_\theta=\frac{\rho_{\theta i}}{r_s},$$
$$\hat{\Phi}=\frac{e_i\Phi}{T_i},\quad \hat{\nu}_{ii}=\frac{Rq}{v_{thi}}\nu_{ii},\quad \hat{\omega}_D=\hat{\rho}_\theta\frac{\sigma\hat{v}}{(1+\epsilon)}\left[\frac{1}{\hat{L}_q}\left\langle\frac{\sqrt{1-yb}}{b}\right\rangle_\theta-\frac{1}{2}\left\langle\frac{1}{\hat{L}_B}\frac{(2-yb)}{b\sqrt{1-yb}}\right\rangle_\theta\right],$$

we obtain the dimensionless equation for $\bar{G}_0$:

$$-m\left[\frac{\hat{p}}{\hat{L}_q}\Theta(y_c-y)+\hat{\omega}_D-\frac{\hat{\rho}_\theta}{2}\left\langle\frac{1}{\hat{v}_\parallel}\frac{\partial\hat{\Phi}}{\partial x}\right\rangle_\theta\right]\left.\frac{\partial\bar{G}_0}{\partial\xi}\right|_p$$
$$+m\left[\frac{\hat{w}^2}{4\hat{L}_q}\sin\xi\,\Theta(y_c-y)-\frac{\hat{\rho}_\theta}{2}\left\langle\frac{1}{\hat{v}_\parallel}\frac{\partial\hat{\Phi}}{\partial\xi}\right\rangle_\theta\right]\frac{\partial\bar{G}_0}{\partial\hat{p}}=\left\langle\frac{1}{\hat{v}_\parallel}\hat{C}_{ii}(\bar{G}_0)\right\rangle_\theta, \tag{18}$$

where Θ is the Heaviside function. Here,

$$\langle\cdots\rangle_\theta=\begin{cases}\frac{1}{2\pi}\oint\cdots d\theta & \text{(passing particles)},\\ \frac{1}{2\pi}\sum_\sigma\sigma\int_{-\theta_b}^{+\theta_b}\cdots d\theta & \text{(trapped particles)},\end{cases} \tag{19}$$

$\hat{C}_{ii}=(Rq/v_{thi})C_{ii}$ and $y_c=1$ corresponds to the trapped/passing boundary in pitch angle space. In the next section we consider the form of the solution in the collisionless limit, then proceed to solve equation (18) in full.

4. Solution for $\bar{G}_0$

In Section 2 we introduced the perturbed flux function Ω describing the magnetic island geometry (see equation (5)). In our present analysis, we introduce a new set of surfaces defined by S:

$$S=\frac{\hat{w}^2}{4\hat{L}_q}\left[\frac{2\left(\hat{p}-\hat{\omega}_D\hat{L}_q\right)^2}{\hat{w}^2}-\cos\xi\right]\Theta(y_c-y)-\hat{p}\hat{\omega}_D\Theta(y-y_c)-\frac{1}{2}\left\langle\frac{\hat{\rho}_\theta}{\hat{v}_\parallel}\hat{\Phi}\right\rangle_\theta. \tag{20}$$

Note that, for $\hat{\Phi}=0$ and $y<y_c$ (passing particles) the constant S surfaces are identical to the constant Ω surfaces, but shifted radially by an amount proportional to $\rho_{\theta i}$. Working with S as the new "radial" coordinate, we can further simplify equation (18) for $\bar{G}_0$, which now takes the form:

$$-m\left[\frac{\hat{p}}{\hat{L}_q}\Theta(y_c-y)+\hat{\omega}_D-\frac{\hat{\rho}_\theta}{2}\left\langle\frac{1}{\hat{v}_\parallel}\frac{\partial\hat{\Phi}}{\partial x}\right\rangle_\theta\right]\left.\frac{\partial\bar{G}_0}{\partial\xi}\right|_S=\left\langle\frac{1}{\hat{v}_\parallel}\hat{C}_{ii}(\bar{G}_0)\right\rangle_\theta, \tag{21}$$

where it should be noted that the differential with respect to ξ is now taken at fixed S. This illustrates that the streamlines lie in surfaces of constant S, not constant Ω. They differ because of the particle orbits - the radial shift of the "drift island" of the constant S contours relative to

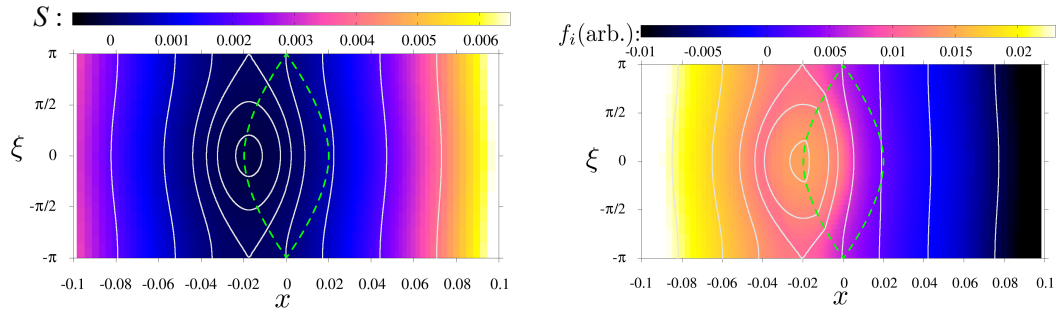

Figure 1. Colour contour plot of S structure in the absence of perturbed electrostatic potential (Left) and full ion distribution function with electrostatic potential (Right) in the $x-\xi$ plane. In both cases solid lines are the S contours, while the dashed line indicates the position of the magnetic island separatrix.

the magnetic island is due to the grad-B and curvature drifts, while the term in Φ arises from $\mathbf{E}\times\mathbf{B}$ drifts.

In Figure 1 (left) we show the contour plot of the S profile in the $x-\xi$ plane, for $\hat{w}=\hat{\rho}_{\theta i}=0.02$, $\hat{L}_q=1.0$, $\lambda/\lambda_c=0.1$, $\hat{v}=1.0$, $\epsilon=0.1$, and $v_{\|}>0$ (likewise for all subsequent figures, unless otherwise indicated). The magnetic island itself is centred about $x=0$. It is clear that the constant S surfaces have the same structure as that of the magnetic island geometry (i.e. constant Ω surfaces), but are radially shifted by $O(\rho_{\theta i})$. In the absence of the electrostatic potential term, this shift is equal and opposite for the $v_{\|}<0$ case. We call this shifted island structure in S the "drift island", whose physical consequence is paramount. In the low collision frequency limit, where we may assume that the term on the right hand side of equation (21) becomes $O(\nu_{ii}Rq/v_{thi})\ll 1$ smaller, it can be shown straightforwardly that the solution for $\bar{G}_0$ is a function S: $\bar{G}_0=\bar{G}_0(S,\boldsymbol{v})$. As we shall see, this leads to the restoration of the density gradient inside the magnetic island, when $\rho_{\theta i}\sim w$. This is what we call the finite orbit width effect, which is distinct from the well known radial transport effect [4].

In Figure 1 (right), we present the colour contour plot of the full perturbed ion distribution function f_i in the $x-\xi$ plane, obtained by solving equation (21) numerically for $\nu_*=0.01$. The electrostatic potential is determined via quasineutrality using the present result for ions and the electron response of [6]. The plot clearly shows that the colour contours of f_i are well-aligned with the contour lines of S, and they are radially shifted relative to the island separatrix. As expected, f_i is indeed a function of S to leading order, and the radial shift of the profile is $O(\rho_{\theta i})$. As shown in Figure 2 (left), flattening of the density gradient inside the magnetic island is well-preserved for $\rho_{\theta i}\ll w$ but is almost absent for $\rho_{\theta i}\sim w$. The restoration of the density gradient across the magnetic island is precisely the result of the shift in the drift islands; because the flat spots in the shifted distribution functions for $\sigma=\pm 1$ no longer align when $w\sim\rho_{\theta i}$; the summation over σ causes the gradient to be maintained across the island. Specifically, the $\sigma=+1$ solution for f_i has a gradient where the $\sigma=-1$ solution is flattened, and vice versa (see Figure 2 (right)). On the other hand, if $\rho_{\theta i}\ll w$, then the flat regions for $\sigma=\pm 1$ do align to a large extent and the density gradient is flattened inside the magnetic island.

For electrons, the strong parallel flow tends to keep the density flattened across the magnetic island width, even for small islands (i.e. $\rho_{\theta i}\sim w$, but $\rho_{\theta e}\ll w$). However, the electron distribution function depends on the electrostatic potential as well, in such a way as to satisfy quasineutrality. Therefore the full density, including the Boltzmann factor, takes the form given in Figure 2 for both ions and electrons. This physics has consequences for the structure of the electrostatic potential (Figure 3). When $\rho_{\theta i}\ll w$, the potential is constant on the perturbed flux

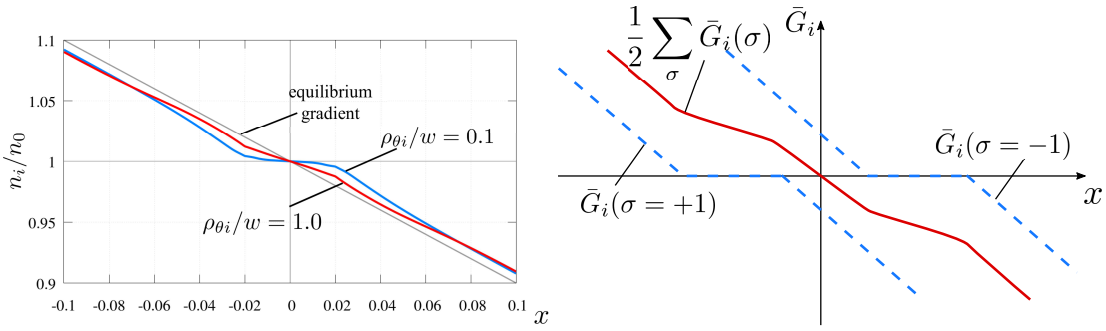

Figure 2. Left: Ion density profile for $w/r = 0.02$, $\rho_{\theta i}/w = 0.1$ (blue) and $\rho_{\theta i}/w = 1.0$ (red) across the island O-point ($\xi = 0$). Even for small $\rho_{\theta i}$ there is a partial restoration of the flattened density gradient, and the flattening is almost entirely gone for $\rho_{\theta i} \sim w$. Right: Schematic drawing depicting the radial shifts of the ion distribution function resulting in the restoration of the density gradient.

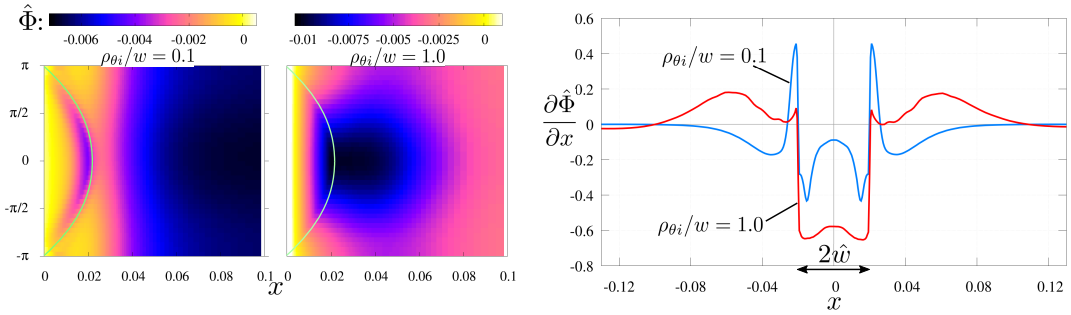

Figure 3. Left: Colour contour plot of the normalised electrostatic potential $\hat{\Phi}$ in the $x - \xi$ plane, for $\rho_{\theta i}/w = 0.1$ (left half) and $\rho_{\theta i}/w = 1.0$ (right half). Solid lines indicate the position of the island separatrix. Right: Plot of the electrostatic potential radial gradient against x across the island O-point. A substantial potential gradient is maintained across the island width.

surfaces, as expected from previous theories. However, when $\rho_{\theta i} \sim w$, this is no longer the case. Furthermore, the region inside the island retains a substantial potential gradient, consistent with the picture described above. The same is true for the ion parallel flow profile, as shown in Figure 4. For large islands, the flow is a perturbed flux quantity, with a well defined boundary layer flow in the vicinity of the island separatrix. Conversely, for a small island the flow is no longer constant on the flux surfaces, and the boundary layer structure is completely lost.

5. Contributions to Island Evolution

We now consider the contribution to the island evolution originating from the perturbed current, localized in the vicinity of the rational surface, Δ'_{loc} (which includes the bootstrap current contribution Δ_{bs}). We project out the component that is constant on the flux surface,

$$\langle J_\parallel \rangle_\Omega = \frac{1}{B_0} \sum_j n_j e_j \left\langle \langle B u_{\parallel j} \rangle_\theta \right\rangle_\Omega, \tag{22}$$

from which Δ'_{loc} can be calculated using the dispersion relation derived from Ampère's law:

$$\int_{-\infty}^{\infty} dx \oint d\xi \, \langle J_\parallel \rangle_\Omega \cos\xi = \frac{c}{32} \frac{w^2}{L_q} \frac{B}{Rq} \Delta'_{loc}, \tag{23}$$

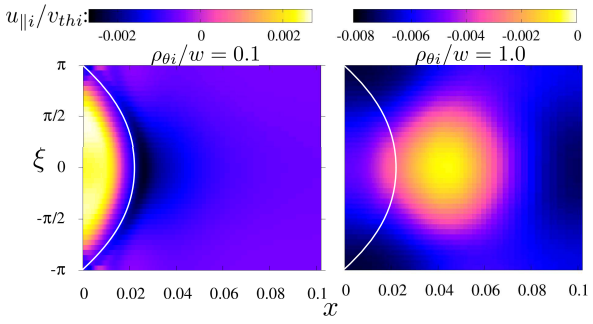

Figure 4. Colour contour plot of the ion parallel flow $u_{\|i}$ on $x - \xi$ plane, for $\rho_{\theta i}/w = 0.1$ (left) and $\rho_{\theta i}/w = 1.0$ (right). Solid lines indicate the position of the island separatrix.

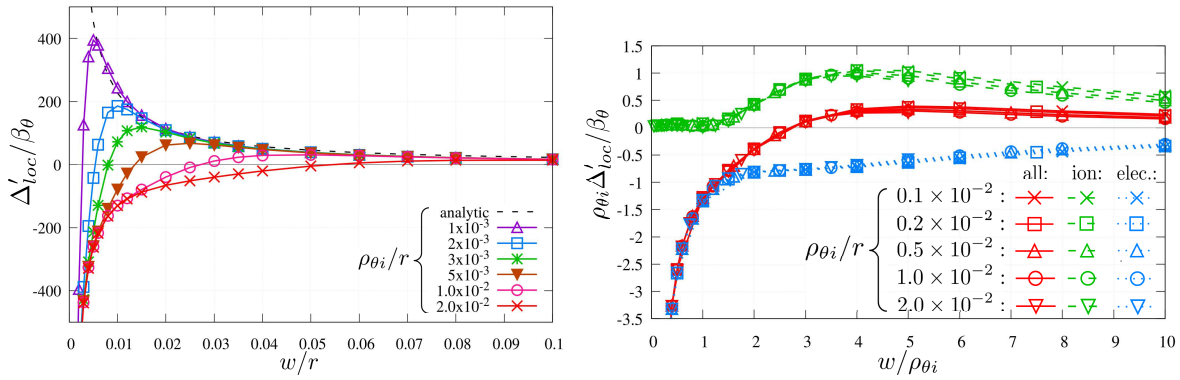

Figure 5. Left: The contribution to the island evolution, Δ'_{loc}, normalised to β_θ, as a function of of $\hat{w}$, for different values of $\rho_{\theta i}$. The black dotted line is the analytic result of [6] for the bootstrap current contribution, for which $\Delta_{bs} \propto 1/w$. Right: Plot of $\rho_{\theta i}\Delta'_{loc}/\beta_\theta$, as a function of $w/\rho_{\theta i}$, for different values of $\rho_{\theta i}$. Red solid curves represent the total contribution, while green dash and blue dotted curves correspond to ion and electron contributions respectively.

Figure 5 (left) shows the results for Δ'_{loc} normalized to $\beta_\theta = 2\mu_0 p/B_\theta^2$ as a function of w for a range of values of $\rho_{\theta i}$. For large $w \gg \rho_{\theta i}$, Δ'_{loc} tends to the asymptotic value ($\lim \rho_{\theta i}/w \to 0$) expected from previous analytic theories for the bootstrap drive [2, 6], which is represented by the dashed line. However, for small island widths comparable to $\rho_{\theta i}$, we see that the impact of the shifted drift islands is to reduce the bootstrap drive. For even smaller island widths, Δ'_{loc} becomes negative. This is a rather remarkable result, as it means that the effect of the current perturbation is to heal the island and therefore represents new threshold physics that cannot be explained by a reduced bootstrap drive alone. For larger $\rho_{\theta i}$, the peak value in Δ'_{loc} decreases substantially, hence suppressing the bootstrap drive for the island growth. The critical island width, w_c, increases linearly with $\rho_{\theta i}$: it can be fitted by $w_c \simeq 2.76\rho_{\theta i}$. Experimental observations support this linear relationship [16], though the coefficient we derive is somewhat larger than the result obtained from experiments.

Finally, we consider the physics underpinning the stabilization of small islands, $w \lesssim \rho_{\theta i}$. Figure 5 (right) shows the plots of $\rho_{\theta i} \times \Delta'_{loc}/\beta_\theta$ vs. $w/\rho_{\theta i}$ (red solid lines), with separate ion (green dashed lines) and electron (blue dotted lines) contributions. The smallest island considered has the width: $w/\rho_{\theta i} = 1/20$, for which the assumption of small electron poloidal Larmor radius, $\rho_{\theta e} \ll w$, is still approximately valid. It is clear that all cases with different $\rho_{\theta i}/r$ values condense onto a universal set of curves for both the ion and electron contributions.

This is a consequence of the parallel flows being proportional to $\rho_{\theta i,e}$, as predicted by analytic neoclassical theory. An important point to address is that, as $w \to 0$, the ion contribution to Δ'_{loc} tends to zero. This is consistent with the density gradient (and therefore bootstrap current) being unperturbed in this limit (as found in the PIC simulations of [19]). Indeed, we expect that when the island width is much less than the ion banana width, the ions will average over the perturbed electromagnetic fields associated with the island. Electrons still respond to the perturbed fields, and we see from Figure 5 (right) that it is their response that provides the stabilizing contribution, which is not the standard result for the bootstrap current contribution. We conclude that it is the response of the electrons to the electrostatic potential, required for quasi-neutrality, that creates the stabilizing contribution to the current density. For even smaller islands with a width $w \lesssim \rho_{\theta e}$, however, the electron response needs to be treated in the same framework as that for the ion response presented here. Going further, as $w \to 0$, i.e. $w \ll \rho_{\theta i}$ and $w \ll \rho_{\theta e}$, then we anticipate the finite Larmor radius effect to start dominating. Investigating this in toroidal geometry would be a challenging task, but is in the scope of our future work.

6. Conclusion

We have presented a new drift kinetic theory for the response of ions to small magnetic island perturbations in a tokamak plasma, as well as the implications for the NTM threshold physics. The effects of guiding centre drifts and finite orbit width effect are substantial. The profile of the perturbed ion distribution function is radially shifted relative to the magnetic island. This implies that the distribution function is no longer flattened across the magnetic island, but instead across a radially shifted drift island. This shift is important for small islands $w \sim \rho_{\theta i}$, in which case a pressure gradient is maintained inside the magnetic island even if cross-field transport is neglected. The bootstrap current drive for the NTM is then suppressed with the flows dominated by the electron physics. The response of the electrons to the perturbed electrostatic potential is such that it tends to heal islands of width w below a critical width w_c, thus providing a threshold for NTM growth. We find that, in the absence of other effects, the critical island width scales linearly with $\rho_{\theta i}$: $w_c \sim 2.76\rho_{\theta i}$.

The new physics of the finite ion orbit width effect is important for a complete theory of the neoclassical tearing mode threshold and, in particular, for designing the NTM control system for ITER. For our theory to fully quantify the NTM theory, we need to address additional physics including the accuracy of the analytic electron response employed here, the finite ion Larmor radius effect, particularly in the vicinity of the island separatrix, as well as the impact of the island propagation frequency that leads to the ion polarization current. Nevertheless, this work gives a new insight into the physics of small magnetic islands and the NTM threshold.

Acknowledgments

This work was supported by the UK Engineering and Physical Sciences Research Council, grant number EP/N009363/1. Numerical calculations were performed using the ARCHER computing service through the Plasma HEC Consortium EPSRC Grant Number EP/L000237/1, as well as on EUROfusion High Performance Computer (Marconi-Fusion).

References

[1] Rutherford P H 1973 *Physics of Fluids* **16** 1903–1908
[2] Carrera R, Hazeltine R D and Kotschenreuther M 1986 *Physics of Fluids* **29** 899–902
[3] Chang Z, Callen J D, Fredrickson E D, Budny R V, McGuire C C H K M, Zarnstorff M C and TFTR group 1995 *Physical Review Letters* **74** 4663–4666
[4] Fitzpatrick R 1995 *Physics of Plasmas* **2** 825
[5] Gorelenkov N N, Budny R V, Chang Z, Gorelenkova M V and Zakharov L E 1996 *Physics of Plasmas* **3** 3379
[6] Wilson H R, Connor J W, Hastie R J and Hegna C C 1996 *Physics of Plasmas* **3** 248

[7] Imada K and Wilson H R 2012 *Physics of Plasmas* **19** 032120
[8] Hegna C C and Callen J D 1997 *Physics of Plasmas* **4** 2940
[9] Zohm H 1997 *Physics of Plasmas*
[10] La Haye R J, Isayama A and Maraschek M 2009 *Nuclear Fusion* **49** 045005
[11] Gantenbein G, Zohm H, Giruzzi G, Günter S, Leuterer F, Maraschek M, Meskat J, Yu Q, ASDEX Upgrade Team and ECRH-Group(AUG) 2000 *Physical Review Letters* **85** 1242
[12] Isayama A, Kamada Y, Ide S, Hamamatsu K, Oikawa T, Suzuki T, Neyatani Y, Ozeki T, Kajiwara K and the JT-60 team 2000 *Plasma Physics and Controlled Fusion* **42** L37
[13] La Haye R J, Günter S, Humphreys D A, Lohr J, uce T C, Maraschek M E, Petty C C, Prater R, Scoville J T and Strait E J 2002 *Physics of Plasmas* **9** 2051
[14] Kolemen E, Welander A S, La Haye R J, Eidietis N W, Humphreys D A, Lohr J, Nraky V, Penaflor B G, Prater R and Turco F 2014 *Nuclear Fusion* **54** 073020
[15] Sauter O, Henderson M A, Ramponi G, Zohm H and Zucca C 2010 *Plasma Physics and Controlled Fusion* **52** 025002
[16] La Haye R J, Prater R, Buttery R J, Hayashi N, Isayama A, Maraschek M E, Urso L and Zohm H 2006 *Nuclear Fusion* **46** 451
[17] Helander P and Sigmar D J 2002 *Collisional Transport in Magnetized Plasmas* Cambridge Monographs on Plasma Physics (Cambridge: Cambridge University Press)
[18] Hirshman S P and Sigmar D J 1981 *Nuclear Fusion* **21** 1079
[19] Poli E, Peeters A G, Bergmann A, Günter S and Pinches S D 2002 *Physical Review Letters* **88** 075001